



BÉZIER CURVES IN THE MODELING OF BOUNDARY GEOMETRY FOR 2D BOUNDARY PROBLEMS DEFINED BY HELMHOLTZ EQUATION

EUGENIUSZ ZIENIUK* and AGNIESZKA BOLTUC†

*Faculty of Mathematics and Physics, University of Białystok
15-887 Białystok, ul. Sosnowa 64, Poland*

**ezieniuk@ii.uwb.edu.pl*

†aboltuc@ii.uwb.edu.pl

Received 11 February 2005

Revised 26 September 2005

The paper uses analytical modification of the classical boundary integral equations (BIEs) for the Helmholtz equation to facilitate the process of practical definition of the boundary geometry. Instead of defining the boundary by means of a boundary integral, the modification makes use of Bézier curves exclusively. As a result, a new parametric integral equation system (PIES) is obtained in which boundary geometry is taken into account in original fundamental boundary solutions. Such boundary definition makes it easy to approximate boundary functions. The proposed method to obtain numerical solution of the PIES for the Helmholtz equation is characterized by high effectiveness.

Keywords: Helmholtz equation; parametric integral equation system (PIES); Bézier curves.

1. Introduction

Solution of practical problems is very often reduced to the solution of boundary problems involving mathematical differential (integral) equations modeling real phenomena. Such problems are typically solved using numerical methods among which the most frequently applied are finite difference method (FDM), finite element method (FEM)¹ and boundary element method (BEM).^{2–5}

All the above methods have one general characteristic in common, i.e. the final solution of boundary problems is reduced to numerical solutions of a number of algebraic equation systems.^{1,5–7} They differ, however, in the way in which these equation systems are obtained and the degree of accuracy they offer.^{7–11} Another common feature the methods share is the fact that they require domain discretization for both FEM and FDM and boundary discretization only in the case of BEM. The methods also show different effectiveness when applied for the solution of complex practical problems.

Their effectiveness can be compared in a number of ways. It is reasonable, however, to take into account such criteria as: (1) amounts of input data necessary to define the investigated problem; (2) the complexity (size) of the obtained system of algebraic equations

approximating the operator equations; (3) accuracy of the obtained solutions; (4) simplicity of the modification of the solved boundary problem. All the above elements have different impacts on the effectiveness of the method depending on the types of boundary problems solved.

Owing to widespread and practical applications of the methods for the solution of a large number of engineering problems as well as the imperfect character of the solutions they offer, the methods used to solve boundary problems require further research. In our work, in spite of quite well-developed FEM and BEM, investigations have been carried out to improve these methods. It appears that a new look at the same differential equations and their mathematical reformulation (but equivalent to the classical one) may frequently lead to a more effective way of their numerical solution.

In our papers, we propose a boundary point method (BPM) to solve boundary problems.¹² The method is based on the parametric integral equation system, which is an effective alternative to the classical boundary integral equation (BIE). The PIES is obtained for the Laplace's equation as a result of the analytical modification of the traditional BIE. The method of the analytical modification of BIE using linear segments to define boundary is presented in Refs. 13 and 14, whereas the modification for the smooth boundary geometry defined by Bézier curves is described in Ref. 15. In the PIES, boundary geometry is mathematically defined by Bézier curves of any given degree, whereas, in practice, only a small number of points lying on the boundary is posed. The number of these points is considerably smaller than the number of nodes that are necessary in BEM to solve the classical BIE. Another advantage of the method is that a modification of a considerable part of the boundary keeping its continuity in the PIES can be affected by means of a small number of de Boor's control points.

The purpose of this paper is to generalize the PIES to the boundary problems defined by the Helmholtz equation. The paper presents an analytical modification of the classical BIE, which results in obtaining a PIES containing original kernels for the Helmholtz equation. The uniqueness of these kernels lies in the fact that they include the boundary geometry defined by Bézier curves of any given degree. The numerical solution of the PIES requires no traditional boundary discretization and is reduced to the approximation of boundary functions exclusively. A number of testing examples are given to illustrate both the effectiveness of boundary definition by boundary points and high accuracy of the results obtained by using the proposed method.

2. Traditional BIE Modification for Helmholtz Equation

The two-dimensional Helmholtz equation is described by the following formula²

$$\frac{\partial^2 \phi}{\partial x_1^2} + \frac{\partial^2 \phi}{\partial x_2^2} + k^2 \phi = 0, \quad \text{for } x \in \Omega, \quad (1)$$

where k is a wave number.

Equation (1) can be solved by means of Green’s formula presented in the following form:

$$\bar{u}(x) = \int_{\Gamma} U^*(x, y) \frac{\partial u(y)}{\partial n} d\Gamma(y) - \int_{\Gamma} \frac{\partial U^*(x, y)}{\partial n} u(y) d\Gamma(y), \quad x \equiv (x_1, x_2), \tag{2}$$

where $\bar{u}(x) = 0.5u(x)$ for $x \in \Gamma$, $\bar{u}(x) = u(x)$ for $x \in \Omega$, $\bar{u}(x) = 0$ for $x \notin \bar{\Omega}$.

In the integral identity (2), the integrand $U^*(x, y)$ is called the fundamental solution for Helmholtz equation. It is described by one of the following formulas⁵:

$$U^*(x, y) = \frac{i}{4} H_0^{(1)}(kr) \quad \text{or} \quad U^*(x, y) = \frac{-i}{4} H_0^{(2)}(kr), \tag{3}$$

where k is wave number. $H_0^{(1)}$ and $H_0^{(2)}$ are the Hankel functions — first and second kind and zero order. Hankel function $H_0^{(1)}$ can be presented in the following form

$$H_0^{(1)}(kr) = J_0(kr) + iY_0(kr). \tag{4}$$

Functions which occur on the right-hand side of the formula are described by

$$J_0(kr) = 1 - \frac{(kr)^2}{4}, \quad Y_0(kr) = \frac{2}{\pi} \left\{ \left(\gamma + \ln \frac{(kr)}{2} \right) \left(1 - \frac{(kr)^2}{4} \right) \right\},$$

where γ is Euler constant ($\gamma = 0.577216\dots$).

If in (2) $x \in \Gamma$, then obtained formula becomes the traditional BIE. In this equation the boundary is defined in formal way by means of the boundary integral. For this reason, for numerical solving of the BIE the boundary equation method is generally used. The method bases on physical division of the boundary into elements and their mathematical description with the help of suitable polynomials.⁵ An alternative for the BIE, in the Laplace’s equation case, is the PIES.¹⁵ The main difference between traditional BIE and the PIES bases on the fact, that in the PIES the boundary geometry is mathematically defined as closed continuous curve. That information is included in the PIES kernels, not in the boundary integral like in the BIE.

Obtaining PIES for the Helmholtz equation requires modification of the traditional Green’s formula (2). Modification can be performed in the same way as in Laplace’s equation.^{13,15,16} After applying Fourier transformation in (2) the following transform is obtained

$$\hat{u}(\xi) = \lambda^{-1}(\xi) \{ \hat{p}(\xi) + i[\xi_1 \tilde{u} \tilde{n}_1(\xi) + \xi_2 \tilde{u} \tilde{n}_2(\xi)] \}, \quad \xi \equiv (\xi_1, \xi_2), \tag{5}$$

where $\lambda^{-1}(\xi) = [\xi_1^2 + \xi_2^2 - k^2]^{-1}$ is an inverse Fourier transform for Helmholtz equation (1), n_m is a direction cosine of normal vector to a boundary Γ , whereas

$$\hat{p}(\xi) = \int_{\Gamma} e^{-i(\xi_1 y_1 + \xi_2 y_2)} p(y) d\Gamma(y), \tag{6}$$

$$\tilde{u} \tilde{n}_m(\xi) = \int_{\Gamma} e^{-i(\xi_1 y_1 + \xi_2 y_2)} n_m(y) u(y) d\Gamma(y), \quad m = 1, 2. \tag{7}$$

In the formula (5) the boundary is defined by means of boundary integrals (6) and (7), which are called the boundary transforms.

2.1. The convolution integral equation system in the domain of Fourier transforms

The integral (7) was used for defining transform function $\tilde{u}\tilde{n}_m(\xi)$ on the boundary Γ . An unknown integrand $u(y)$ in (7) is described by the following Fourier formula

$$u(y) = \frac{1}{4\pi^2} \int_{R^2} e^{i(\omega_1 y_1 + \omega_2 y_2)} \hat{u}(\omega) d\omega, \tag{8}$$

where integrand $\hat{u}(\omega)$ is showed by means of

$$\hat{u}(\omega) = 2\lambda^{-1}(\omega) \{ \tilde{p}(\omega) + i[\omega_1 \tilde{u}\tilde{n}_1(\omega) + \omega_2 \tilde{u}\tilde{n}_2(\omega)] \}, \quad \omega \equiv (\omega_1, \omega_2). \tag{9}$$

Formula (9) is a particular case of formula (5).

After consideration of (9) and (8) in (7), the convolution integral equation system in Fourier transform domain is obtained in the following form:

$$\tilde{u}\tilde{n}_m(\xi) = \int_{R^2} \tilde{K}_m(\gamma_1, \gamma_2) \lambda^{-1}(\omega) \{ \tilde{p}(\omega) + i[\omega_1 \tilde{u}\tilde{n}_1(\omega) + \omega_2 \tilde{u}\tilde{n}_2(\omega)] \} d\omega. \tag{10}$$

The kernel in this equation is a contour integral

$$\tilde{K}_m(\gamma_1, \gamma_2) = \frac{1}{2\pi^2} \int_{\Gamma} e^{i(\gamma_1 y_1 + \gamma_2 y_2)} n_m(y) d\Gamma(y), \quad \gamma_i = \omega_i - \zeta_i, \tag{11}$$

which takes into consideration boundary geometry Γ . In the further contemplations the boundary Γ is divided into n nonlinear segments (but only theoretically).

3. Modeling of the Continuous Boundary by Means of Bézier Segments

In order to define closed boundary geometry, in boundary problems, Bézier curves¹⁷ can be used. Domain Ω , restricted by Bézier segments with assurance of a class of continuity C^1 at points of segment joints, is shown in Fig. 1.

Each segment $\Gamma_k(s)$ ($k = 1, 2, \dots, n$) can be described by means of the following Bézier curves¹⁷

$$\Gamma_k(s) = \left\{ \begin{matrix} y_1 \\ y_2 \end{matrix} \right\} = \left\{ \begin{matrix} \Gamma_k^{(1)}(s) \\ \Gamma_k^{(2)}(s) \end{matrix} \right\} = \sum_{i=0}^n V_i B_{i,n}(s^*), \tag{12}$$

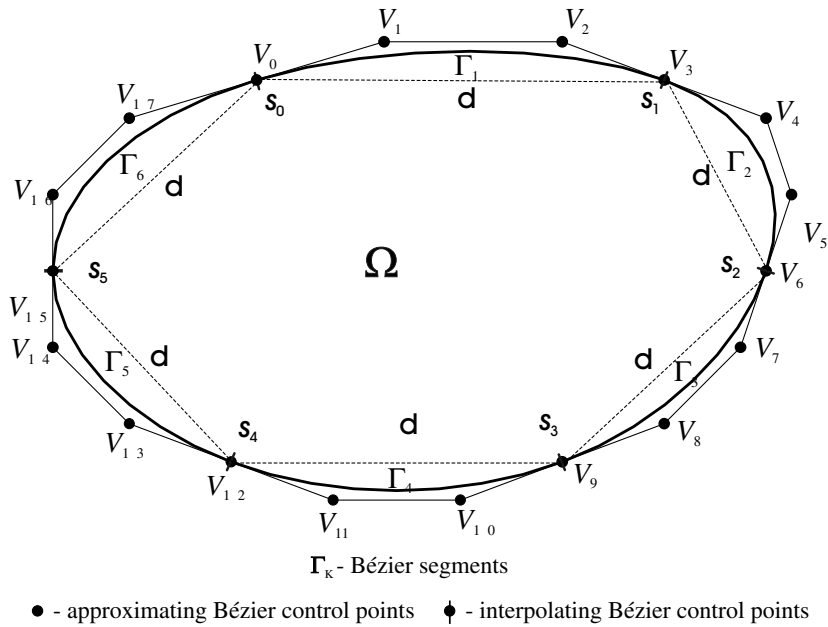


Fig. 1. Modeling of the domain Ω by means of Bézier curves.

where $B_{i,n}(s^*)$ are Bernstein base functions of n degree, and they are written in the following form:

$$B_{i,n}(s^*) = \binom{n}{i} (1 - s^*)^{n-i} s^{*i}, \quad 0 \leq s^* \leq 1,$$

and V_i are Bézier control points.

The kernel (11), after consideration of Bézier segments (12) in it, takes the following form:

$$\tilde{K}_m(\gamma_1, \gamma_2) = \frac{1}{2\pi^2} \sum_{l=1}^n \int_{s_{l-1}}^{s_l} e^{i[\gamma_1 \Gamma_l^{(1)}(s) + \gamma_2 \Gamma_l^{(2)}(s)]} J_l(s) n_m(s) ds, \quad s_{l-1} \leq s \leq s_l, \quad (13)$$

whereas transforms $\tilde{p}(\omega)$, $\tilde{u}\tilde{n}_m(\omega)$ in (10) are presented by means of integrals

$$\tilde{p}_j(\omega) = \sum_{j=1}^n \int_{s_{j-1}}^{s_j} e^{-i[\omega_1 \Gamma_j^{(1)}(s) + \omega_2 \Gamma_j^{(2)}(s)]} p_j(s) J_j(s) ds, \quad (14)$$

$$J_l(s) = \sqrt{(\partial y_1 / \partial s)^2 + (\partial y_2 / \partial s)^2},$$

$$\tilde{u}_k \tilde{n}_m^{(k)}(\omega) = \sum_{k=1}^n \int_{s_{k-1}}^{s_k} e^{-i[\omega_1 \Gamma_k^{(1)}(s) + \omega_2 \Gamma_k^{(2)}(s)]} u_k(s) n_m^{(k)}(s) J_k(s) ds, \quad k = l, j. \quad (15)$$

In that way in boundary integrals the boundary geometry, defined by means of Bézier curves, was considered.

4. PIES for Helmholtz Equation

Considering (14), (15) and (13) in (10) and applying inversion of Fourier transformation into obtained formula, the PIES takes the following form

$$0.5u_l(s_1) = \sum_{j=1}^n \int_{s_{j-1}}^{s_j} \{ \bar{U}_{lj}^*(s_1, s)p_j(s) - \bar{P}_{lj}^*(s_1, s)u_j(s) \} J_j(s) ds, \quad s_{j-1} < s_1, \quad s < s_j. \quad (16)$$

General form of obtained PIES (16) is the same as in the case of the Laplace's equation,¹⁵ the difference is only in kernels \bar{U}_{lj}^* and \bar{P}_{lj}^* . First function \bar{U}_{lj}^* is called the fundamental boundary solution and it is presented in the following form¹⁸

$$\bar{U}_{lj}^*(s_1, s) = \frac{i}{4} H_0^{(1)}(k\eta) \quad \text{or} \quad \bar{U}_{lj}^*(s_1, s) = \frac{-i}{4} H_0^{(2)}(k\eta). \quad (17)$$

Second function from (16) \bar{P}_{lj}^* is called the singular boundary solution

$$\bar{P}_{lj}^*(s_1, s) = \frac{-i}{4\eta} k H_1^{(1)}(k\eta) [\eta_1 n_1(s) + \eta_2 n_2(s)], \quad (18)$$

where $H_1^{(1)}$ are the Hankel functions — first kind and first order.

Function η which occurs in formulas (17) and (18) is described by the following formula

$$\eta = [\eta_1^2 + \eta_2^2]^{0.5}, \quad (19)$$

where $\eta_1 = \Gamma_l^{(1)}(s_1) - \Gamma_j^{(1)}(s)$, $\eta_2 = \Gamma_l^{(2)}(s_1) - \Gamma_j^{(2)}(s)$, and $\Gamma_k(s)$ ($k = 1, 2, \dots, n$) are the boundary segments defined by formula (12).

Boundary solutions (17) and (18), in contrary to classical solutions (2), take into account the boundary geometry in their mathematical formalism. The boundary geometry is defined by means of Bézier curves. Therefore, as a result of modification of the traditional BIE, the PIES was obtained, in which information about boundary geometry is included in kernels of the system.

5. The Solution in the Domain

When we obtain a solution on the boundary using PIES (16), we can obtain a solution in the domain. For this reason integral identity, which use solutions on the boundary obtained earlier, is required. Follow the same way as in Laplace's equation^{14,15} case, identity can be presented in the following form

$$u(x) = \sum_{j=1}^n \int_{s_{j-1}}^{s_j} \{ \hat{U}_j^*(x, s)p_j(s) - \hat{P}_j^*(x, s)u_j(s) \} J_j(s) ds, \quad s_{j-1} < s < s_j. \quad (20)$$

First function \hat{U}_j^* is called the fundamental solution in the domain and it is described by the following formula¹⁸:

$$\hat{U}_j^*(\mathbf{x}, s) = \frac{i}{4} H_0^{(1)}(k\hat{\eta}) \quad \text{or} \quad \hat{U}_j^*(\mathbf{x}, s) = \frac{-i}{4} H_0^{(2)}(k\hat{\eta}). \quad (21)$$

Second function from (20) \hat{P}_j^* is called the singular solution in the domain

$$\hat{P}_j^*(\mathbf{x}, s) = \frac{-i}{4\hat{\eta}} k H_1^{(1)}(k\hat{\eta}) [\hat{\eta}_1 n_1(s) + \hat{\eta}_2 n_2(s)]. \tag{22}$$

Function $\hat{\eta}$, which occurs in the formulas (21) and (22), takes into account the boundary geometry described by Bézier curves, and coordinates of point in the domain, in which the solution is searched. It is described by formula (19)

$$\hat{\eta} = [\hat{\eta}_1^2 + \hat{\eta}_2^2]^{0.5}, \tag{23}$$

where $\hat{\eta}_1 = x_1 - \Gamma_j^{(1)}(s)$, $\hat{\eta}_2 = x_2 - \Gamma_j^{(2)}(s)$, and $\Gamma_k(s)$ ($k = 1, 2, \dots, n$) are boundary segments described by formula (12).

6. Numerical Solving of PIES

The solution of PIES (16) is reduced to finding the unknown functions $u_j(s)$ or $p_j(s)$ on each of the boundary segments of the considered problem. These functions are required in complex approximating expression form

$$u_j(s) = \sum_{k=0}^M \bar{u}_j^{(k)} f_j^{(k)}(s), \quad p_j(s) = \sum_{k=0}^M \bar{p}_j^{(k)} f_j^{(k)}(s), \tag{24}$$

where

$$\bar{u}_j^{(k)} = u_j^{(k)} + i v_j^{(k)}, \quad \bar{p}_j^{(k)} = r_j^{(k)} + i s_j^{(k)}, \tag{25}$$

where $u_j^{(k)}$, $v_j^{(k)}$, $r_j^{(k)}$, $s_j^{(k)}$ are the unknown coefficients on segment j , k is the number of the coefficients, whereas $f_j^{(k)}(s)$ are global base functions on each segment. We can use any orthogonal polynomials¹⁹ as base functions in the proposed algorithm. Generally $f_j^{(k)}(s)$ are presented in the following form

$$f_j^{(k)}(s) = \{P_k(s), H_k(s), L_k(s), T_k(s)\}, \tag{26}$$

where

$P_k(s)$ are the Legendre polynomials, $H_k(s)$ are the Hermite polynomials,
 $L_k(s)$ are the Laguerre polynomials, and $T_k(s)$ are the Chebyshev polynomials.

After insertion of (24) into (16), the PIES is obtained. The PIES written down for all collocation nodes takes the matrix form

$$[H]\{\bar{u}_j\} = [G]\{\bar{p}_j\}, \tag{27}$$

where

$$\begin{aligned}
 [h_{lj}] &= 0.5\delta_{lj} \sum_{k=0}^M f_j^{(k)}(s) + \sum_{k=0}^M \int_{s_{j-1}}^{s_j} \bar{P}_{lj}^*(s_1, s) f_j^{(k)}(s) J_j(s) ds, \\
 [g_{lj}] &= \int_{s_{j-1}}^{s_j} \bar{U}_{lj}^*(s_1, s) f_j^{(k)}(s) J_j(s) ds.
 \end{aligned}
 \tag{28}$$

The unknown functions of complex approximating series (24) are described by

$$\{\bar{u}_j\} = \{u_j^{(k)}\} + i\{v_j^{(k)}\}, \quad \{\bar{p}_j\} = \{r_j^{(k)}\} + i\{s_j^{(k)}\}.
 \tag{29}$$

After consideration of (29) in the matrix equation (27), each segment can be presented in the following form

$$\begin{bmatrix} H_1 & -H_2 \\ H_2 & H_1 \end{bmatrix} \begin{Bmatrix} u_j^{(k)} \\ v_j^{(k)} \end{Bmatrix} = \begin{bmatrix} G_1 & -G_2 \\ G_2 & G_1 \end{bmatrix} \begin{Bmatrix} r_j^{(k)} \\ s_j^{(k)} \end{Bmatrix},
 \tag{30}$$

where

$$H_1 = \text{Re } h_{ij}, \quad H_2 = \text{Im } h_{ij}, \quad G_1 = \text{Re } g_{ij}, \quad G_2 = \text{Im } g_{ij}.$$

Unknown coefficients $u_j^{(k)}$, $v_j^{(k)}$ or $r_j^{(k)}$, $s_j^{(k)}$ are solutions of algebraic equation system (27). Multiplication of coefficients by base functions leads to continuous solution on each segment.

7. Tested Examples and Discussion

Effectiveness of proposed algorithm for numerical solving of the PIES was tested on various examples with different analytical solutions and in the different domains. Obtained solutions, for various number of expressions in the complex approximating series (24), arrangement of collocation nodes and value of wave number k , were compared with the exact and other numerical results.

7.1. Example 1

In the first example, circular domain (Fig. 2) defined by Bézier curves of the third degree was considered. For its defining only interpolating boundary points V_i ($i = 0, 3, 6, 9, 12, 15, 18, 21$) were applied. The Dirichlet boundary conditions were set. They are calculated on the basis of analytical solution showed by function

$$u = -i \frac{\cos[k(1-x)]}{\sin(k)}.
 \tag{31}$$

In order to solve the following example $k = 1$ was taken. Solutions presented here refer to one cross-section: $y = 0$ and $-0.45 \leq x \leq 0.45$.

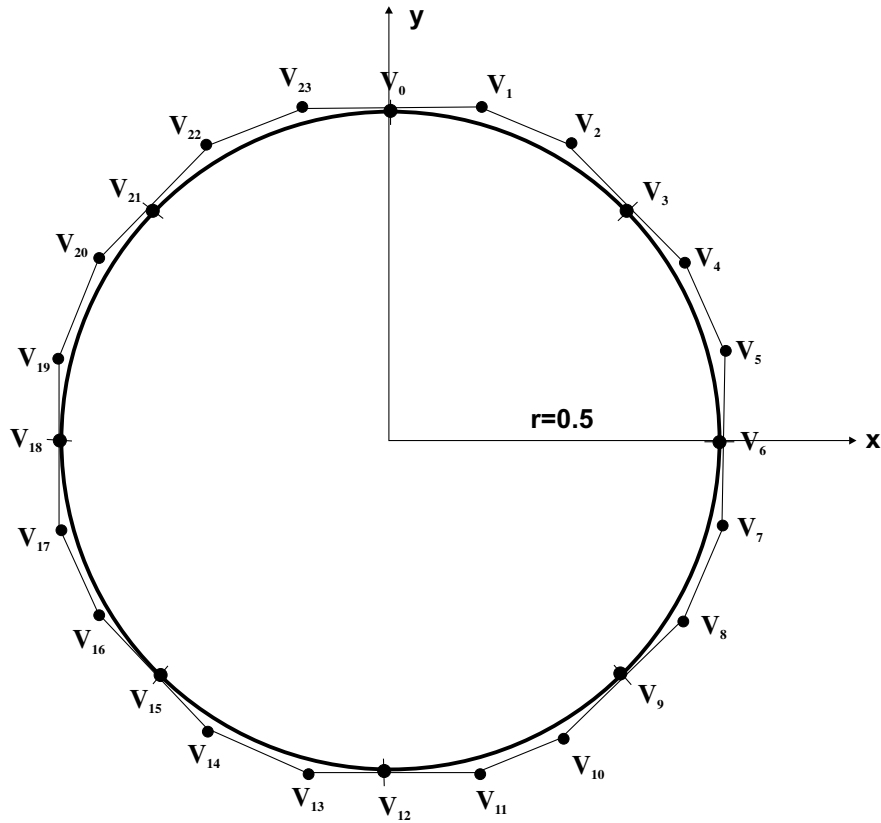


Fig. 2. Circular domain defined by Bézier curves of the third degree.

The influence of the collocation nodes placement and the number of terms in the approximating series (24) were analyzed. The test has been carried out taking into account 2, 3, 4 and 5 terms ($M = 1, 2, 3, 4$) of the approximating series (24), and three ways of arrangement of collocation nodes:

- (1) placement uniformity,
- (2) placing of nodes at points corresponding to the roots of the Chebyshev polynomials,
- (3) placement of two collocation nodes at a distance of 0.1 from the boundary with all the remaining nodes being placed in a uniform way.

The first stage of the tests has been carried out taking into account four terms ($M = 3$) of the approximating series. The relative error of obtained results is shown in Fig. 3. Only imaginary part of solution is presented below, because analytical value of the real part amounts to 0.

As seen in the diagrams, the proposed method gives very accurate results for all arrangements of the collocation nodes. The greatest relative error occurs when the collocation points are placed at sites corresponding to Chebyshev polynomial. Most effective is the case, in which the collocation nodes are evenly placed.

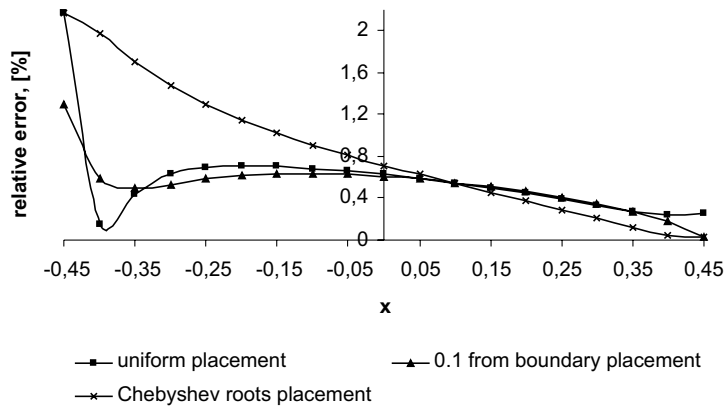


Fig. 3. Error values for imaginary part of solution for different placements of collocation nodes.

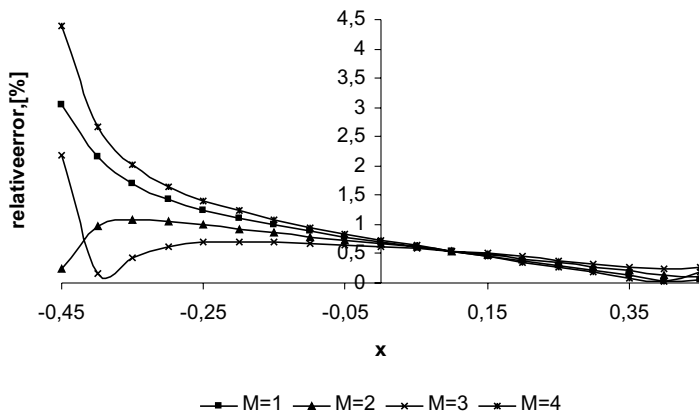


Fig. 4. Error values for imaginary part of solution for different number of expressions in the approximating series.

The next stage of tests refers to investigate an influence of number of expressions in the approximating series on the accuracy of the results. The tests were performed on the collocation nodes placement, which gave the most accurate results. 2, 3, 4 and 5 expressions of the approximating series were considered. The results are shown in Fig. 4.

The results for ($M = 1, 2, 3, 4$) expressions of the approximating series are practically the same and at the same time very close to the analytical results (Fig. 4). The tests showed that smallest relative error occurs when four expressions ($M = 3$) of the approximating series were used. The greatest differences between exact and numerical results occur where $M = 4$ was considered.

7.2. Example 2

In the second example, the Helmholtz equation (1) in an elliptical domain with the Dirichlet boundary conditions was solved. Considered domain is shown in Fig. 5. Like in example 1 for

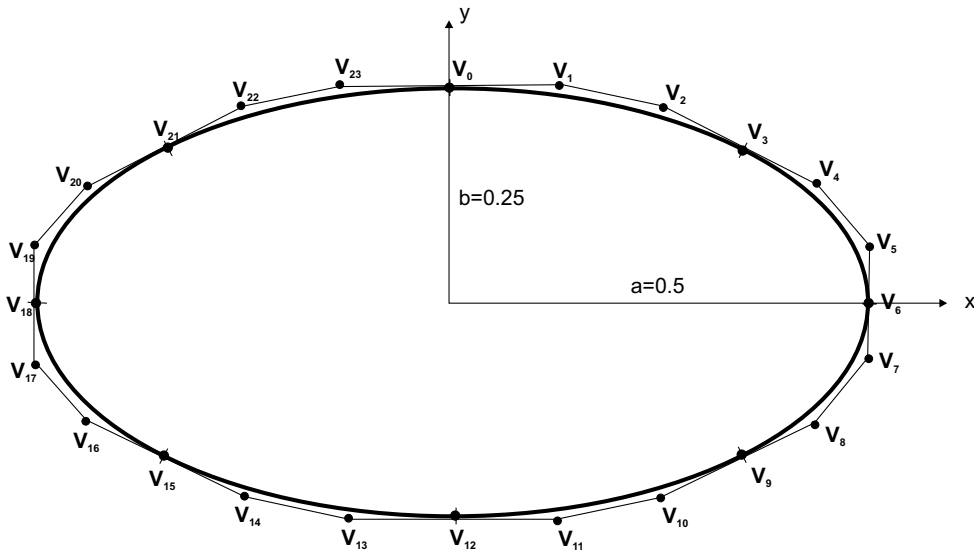


Fig. 5. Investigated domain defined by Bézier curves of third degree.

boundary geometry defining only interpolating Bézier control points were used. For exact defining of boundary geometry, number of those points is much less than the number of nodes in BEM case. The analytical solution is shown by function⁷

$$u = \exp ik\{x \cos \alpha + y \sin \alpha\}. \tag{32}$$

In order to solve the following example $\alpha = 0^\circ$ was taken. Different values of k ($k = 0.25, 0.5, 0.75, 1$) were considered.

In order to test the accuracy of the method, solutions in the different cross-sections of the domain were analyzed. Each solution is compared with exact result. Owing to the fact that there is some regularity of the solution obtained in all individual cross-sections of the domain, the solutions presented here refer only to one cross-section.

Four terms ($M = 3$) of the approximating series (13) and evenly placement of collocation nodes were considered.

The relative error for the real and imaginary parts of solution in the domain for different k values is shown in Figs. 6(a) and 6(b).

As shown in Figs. 6(a) and 6(b), the value of relative error depends on considered value of wave number k . Value of the relative error increases with increasing value of k . The proposed method gives very small relative errors for all considered cases (less then 0.13% for real part of the solution and 0.28% for the imaginary part).

7.3. Example 3

In the third example a square domain (Fig. 7) with the Dirichlet boundary conditions was considered. Investigated domain is defined by segments of the first degree. Defining is

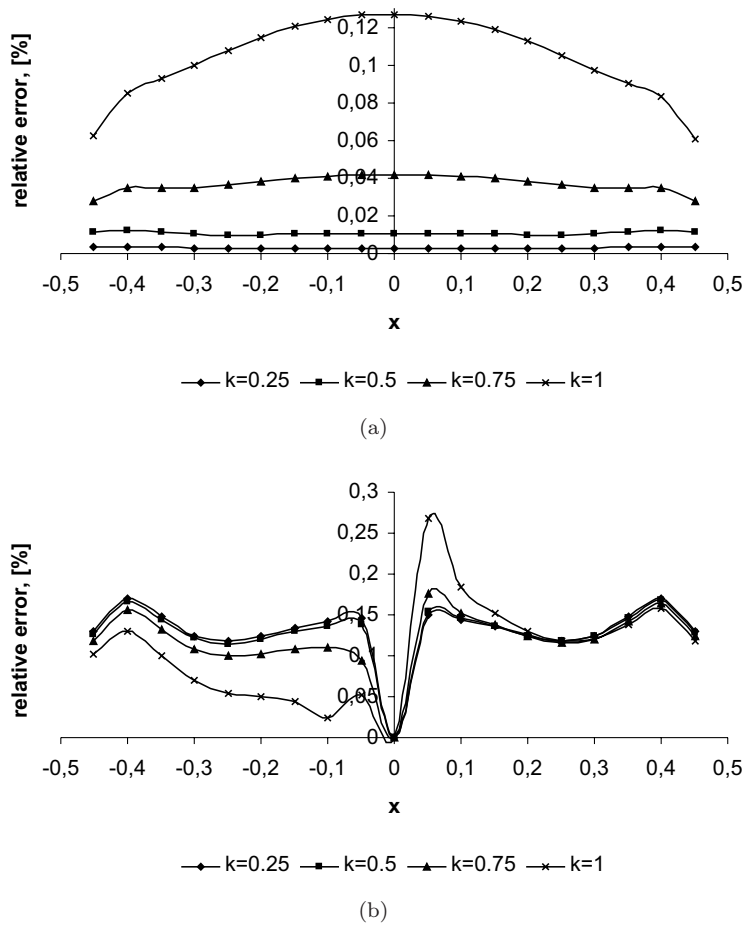


Fig. 6. (a) Error values for real part of solution. (b) Error values for imaginary part of solution.

reduced to set only four corner points P_i ($i = 0, 1, 2, 3$). In the BEM case, the boundary is divided into boundary elements (with greater number of nodes). The analytical solution of Helmholtz equation (1) is shown by function (32) from second example. In order to solve the following example $\alpha = 0^\circ$ and $k = 0.25$ was taken.

In order to test the accuracy of the results obtained from the PIES, they were compared with the ones obtained from BEM and with analytical results. The comparison is shown in Table 1.

The solutions obtained from the PIES give the smallest errors. In order to obtain those results, eight algebraic equations were solved. The next advantage of proposed method (modified BEM) is that for obtaining great accuracy, the same or even smaller algebraic equation system was solved. It is related with the shorter time of calculation and the smaller number of computer storage used for numerical solving of boundary problems. The smaller number of input data for boundary geometry definition is also required.

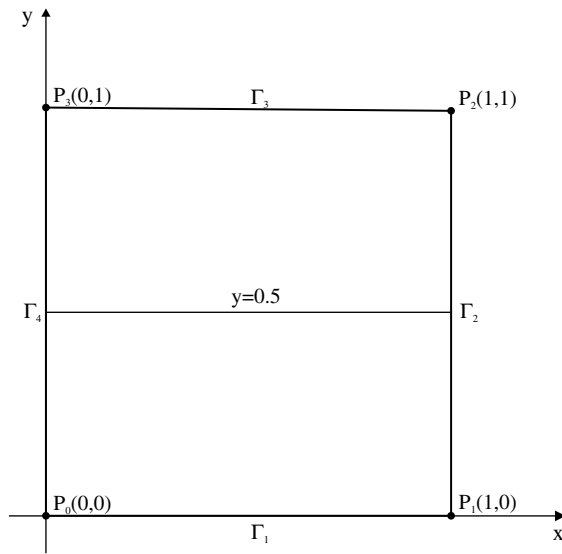


Fig. 7. Investigated domain defined by Bézier curves of first degree.

Table 1. Comparison of the results obtained from BEM and PIES with the exact results.

x	y	PIES (8)		BEM (8)	
		$ \varepsilon_u $, % Re	$ \varepsilon_u $, % Im	$ \varepsilon_u $, % Re	$ \varepsilon_u $, % Im
0.1	0.5	0.14599724	5.03170777	0.03256180	11.5747893
0.2	0.5	0.00703483	1.77847948	0.04057675	3.72789163
0.3	0.5	0.00900713	0.75538433	0.04821735	1.59977573
0.4	0.5	0.01157435	0.28208655	0.05619728	0.65250360
0.5	0.5	0.01468127	0.01422372	0.06416737	0.06876564
0.6	0.5	0.01841456	0.16385879	0.07120737	0.32312202
0.7	0.5	0.02310681	0.30318077	0.07774126	0.59552782
0.8	0.5	0.02934268	0.42566671	0.08750199	0.85854681
0.9	0.5	0.17697143	0.38620049	0.10618725	1.22615861
Average relative error		0.04845892	1.01564318	0.0.0649287	2.2918979

(in parentheses — number of solved algebraic equations)

8. Conclusions

In the paper, classical boundary integral equations have been modified to obtain a PIES for boundary problems defined by a 2D differential Helmholtz equation. In the PIES, the boundary geometry is not defined by the boundary integral as in BIE (i.e. in a very general way), it is only included in the original kernels obtained for the PIES and defined by Bézier curves. This makes it possible to effectively pose boundary geometries with the help of a

small number of boundary points. Posing only boundary points in the PIES is equivalent to the definition of the complete boundary geometry in a continuous way, not a discrete one, as in the case of FEM used to solve the PIES. The above follows from the analytical and continuous boundary definition by Bézier curves in the fundamental boundary solutions obtained. Hence the PIES is no longer defined on the boundary but on the straight line in the parametric system of reference for any given geometry.

As a result of the proposed modification of the classical BIE, a PIES in which the boundary geometry was analytically included in its mathematical formalism, was obtained. Such boundary definition offers greater possibilities of more effective concentration on the approximation process of boundary functions, i.e. solution of the PIES. Thus, we can state that in the PIES there is no necessity of simultaneous application of the approximation of the boundary geometry and boundary functions, unlike in BIE.

Finally, the solution of the PIES is reduced to the approximation of boundary functions entirely. The use of the pseudospectral method to solve the PIES, as shown in the example, is characterized by high effectiveness and accuracy of the solutions. The obtained PIES and the proposed method of its solution constitutes an effective alternative method for the classical BEM.

References

1. O. Zienkiewicz, *The Finite Element Methods* (McGraw-Hill, London, 1977).
2. M. C. Au and C. A. Brebbia, Diffraction of water waves for vertical cylinders using boundary elements, *Appl. Math. Model.* **7** (1983) 106–114.
3. J. T. Chen, K. H. Chen and C. T. Chen, Adaptive boundary element method of time-harmonic exterior acoustics in two dimensions, *Comput. Methods Appl. Mech. Eng.* **191** (2002) 3331–3345.
4. J. T. Chen, Recent development of dual BEM in acoustic problems, *Comput. Methods Appl. Mech. Eng.* **188** (2000) 833–845.
5. C. A. Brebbia, J. C. F. Telles and L. C. Wrobel, *Boundary Element Techniques, Theory and Applications in Engineering* (Springer-Verlag, New York, 1984).
6. S. Amini and S. M. Kirkup, Solution of Helmholtz equation in the exterior domain by elementary boundary integral methods, *J. Comput. Phys.* **118** (1995) 208–221.
7. F. Q. Hu, A spectral boundary integral equation method for the 2D Helmholtz equation, *J. Comput. Phys.* **120**(2) (1995) 340–347.
8. W. Yeih, J. T. Chen, K. H. Chen and F. C. Wong, A study on the multiple reciprocity method and complex-valued formulation for the Helmholtz equation, *Adv. Eng. Softw.* **29**(1) (1998) 1–6.
9. S. Marburg and S. Schneider, Influence of element types on numeric error for acoustic boundary elements, *J. Comput. Acoust.* **11**(3) (2003) 363–386.
10. M. T. Liang, J. T. Chen and S. S. Yang, Error estimation for boundary element method, *Eng. Anal. Boundr. Elem.* **23** (1999) 257–265.
11. A. J. B. Tadeu, L. Godinho and P. Santos, Performance of the BEM solution in 3D acoustic wave scattering, *Adv. Eng. Softw.* **32** (2001) 629–639.
12. E. Zieniuk, Boundary points methods us non-elements method for solving two-dimensional Laplace's equation, in *Symulacja w badaniach i rozwoju*, eds. A. Tylikowski and A. Grzyb (Kraków, 2004), pp. 423–430 (in polish).

13. E. Zieniuk, Potential problems with polygonal boundaries by a BEM with parametric linear functions, *Eng. Anal. Boundr. Elem.* **25**(3) (2001) 185–190.
14. E. Zieniuk, A new integral identity for potential polygonal domain problems described by parametric linear functions, *Eng. Anal. Boundr. Elem.* **26**(10) (2002) 897–904.
15. E. Zieniuk, Bézier curves in the modification of boundary integral equations (BIE) for potential boundary-value problems, *Int. J. Sol. Struct.* **40**(9) (2003) 2301–2320.
16. E. Zieniuk, Simple-layer potential with boundary modelling by B-spline curves for Helmholtz equations, *Structures–Waves–Biomedical Eng.* **X** (2001) 91–100.
17. N. M. Mortenson, *Geometric Modelling* (John and Sons, Chichester, 1985).
18. E. Zieniuk, Linear-segmented modification of the boundary integral equations for Helmholtz equation, *Struct. Acoust. Vibr. Technol.* **8** (1999) 115–118 (in polish).
19. D. Gottlieb and S. A. Orszag, *Numerical Analysis of Spectral Methods* (SIAM, Philadelphia, 1997).

Copyright of *Journal of Computational Acoustics* is the property of World Scientific Publishing Company and its content may not be copied or emailed to multiple sites or posted to a listserv without the copyright holder's express written permission. However, users may print, download, or email articles for individual use.